Coalescence production of light nuclei in HIC

Che Ming Ko
Texas A&M University

- ❑ Introduction
- ❑ The coalescence model
- ❑ Coalescence vs statistical models
- ❑ Coalescence vs transport models
- ❑ Coalescence production of hypertriton
- ❑ Coalescence production of light nuclei production in small systems
- ❑ Effect of density fluctuations on light nuclei production
- ❑ Summary

The coalescence model

- 1960s

  1) Butler and Pearson, PR 129, 836 (1963): Two nucleons coalescence into a deuteron with the nuclear matter acting as a catalyzer. In second-order perturbation theory,

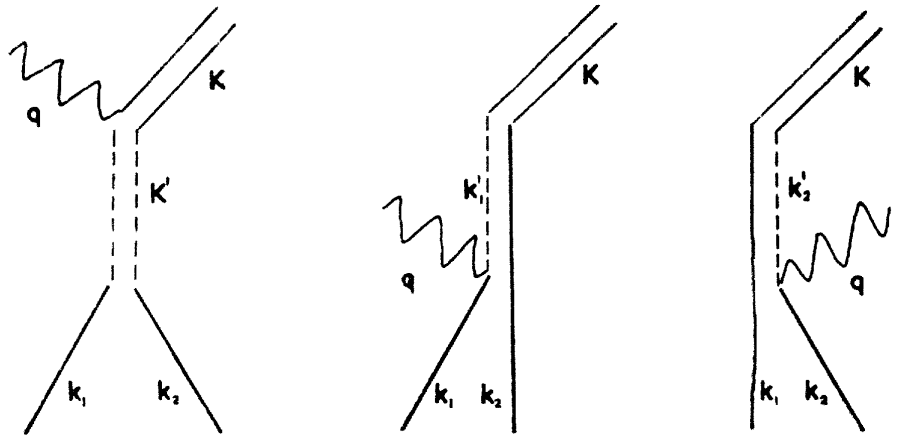

$$N_d(\mathbf{K}) \propto [N_p(\mathbf{K}/2)]^2$$

  2) Schwalzschild and Zupancic, PR 129, 854 (1963): The deuteron-to-proton ratio is governed by the probability of finding a neutron within a small sphere of radius ρ around the proton in momentum space

$$dN_d(K)/dN_p(K) \propto \frac{4\pi\rho^3}{3}$$

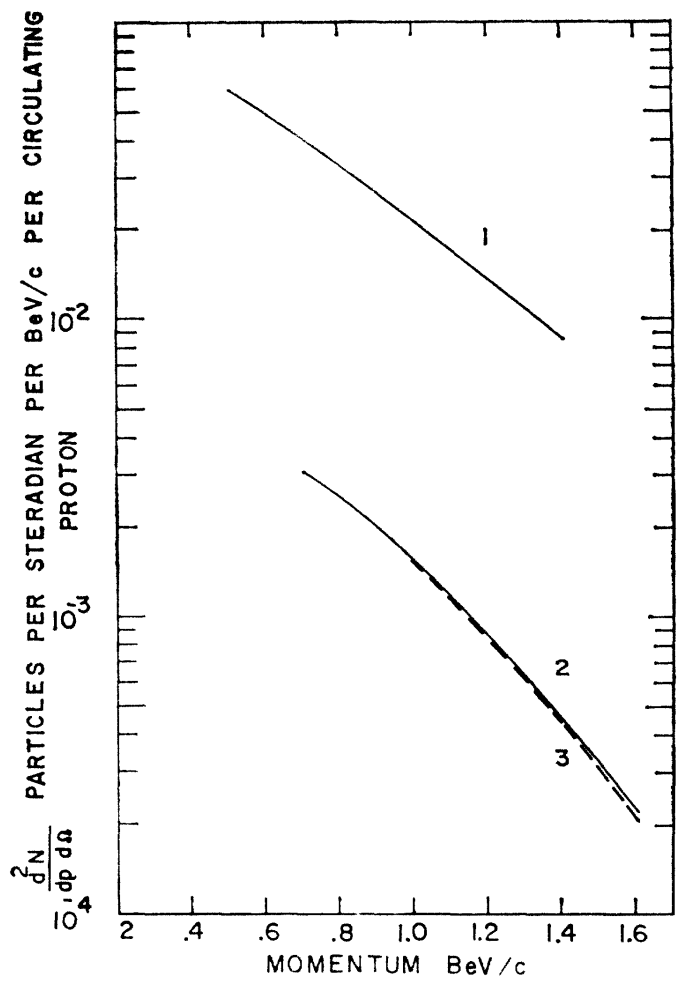

FIG. 3. A comparison of the observed and calculated momentum distributions for deuterons produced from a Be target at an angle of 45° in the laboratory system by protons with incident energy 30 BeV. Curves 2 and 3 are the observed and the calculated deuteron distribution (34). Curve 1 is the experimental distribution of cascade protons used to calculate (34). The experimental data are those of Fitch *et al.* (reference 3).

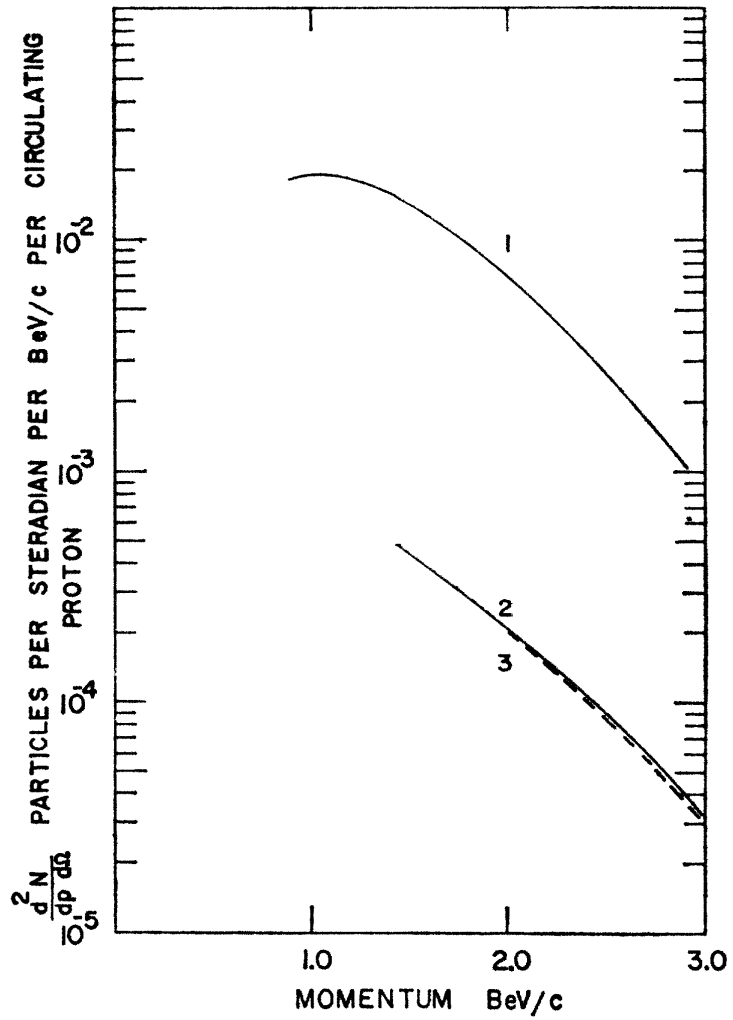

FIG. 4. As in Fig. 3, the deuterons are produced from a Be target at an angle of 30° in the laboratory system by protons with incident energy 30 BeV. The curves are labeled as in Fig. 3, and the experimental results are those of Schwarzschild and Zupančič (reference 6).

Coalescence production of light nuclei at Bevalac

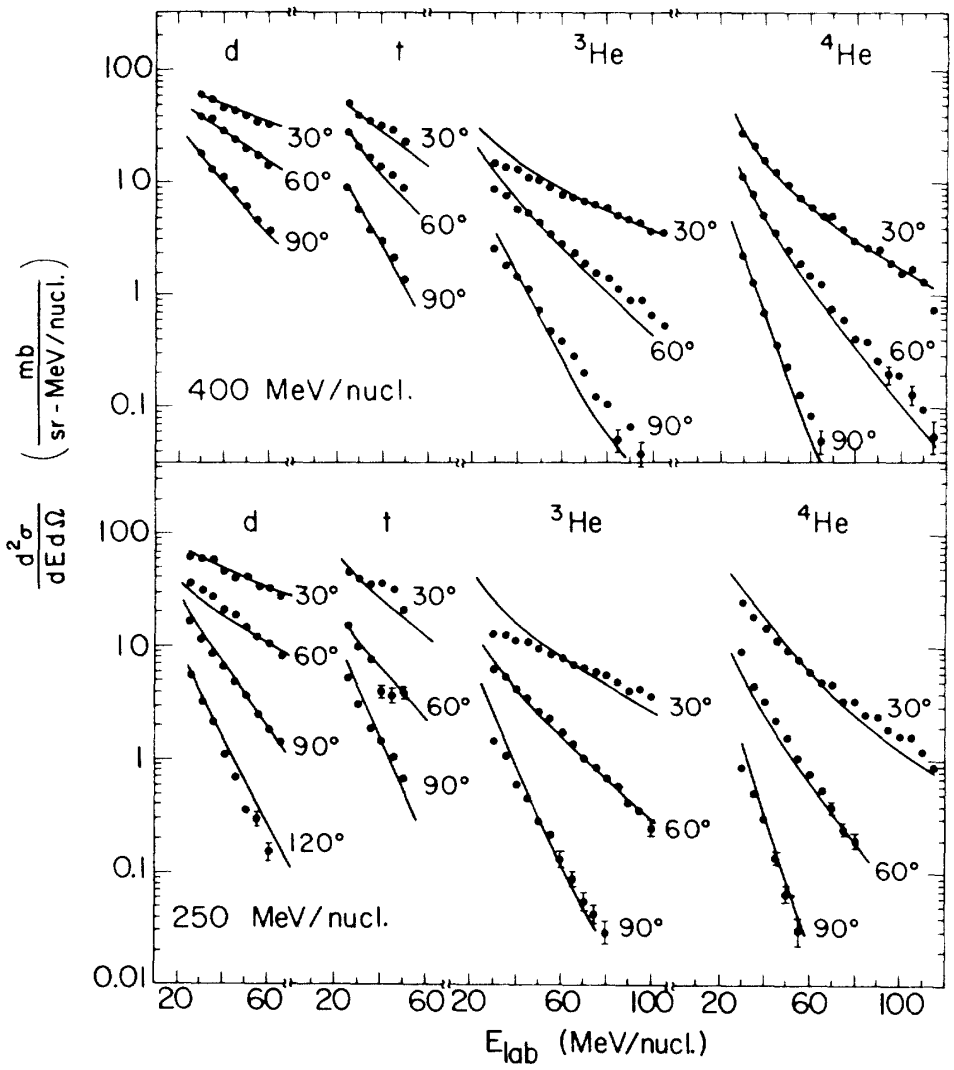

FIG. 3. Experimental points and calculated lines for the double-differential cross sections of fragments from the irradiation of uranium by ^{20}Ne ions at 250 and 400 MeV/nucleon.

Gutbrod et al., PRL 37, 667 (1976)

$$E_A \frac{d^3 N_A}{dp_A^3} = B_A \left(E_p \frac{d^3 N_p}{dp_p^3} \right)^A$$

$$B_A = \left(\frac{4\pi}{3} p_0^3 \right)^{A-1} \frac{M}{m^A}, \; p_A = A p_p$$

Coalescence radius p_0 (MeV)

Nuclei	250	400
d	126	129
t	140	129
^{3}He	135	129
^{4}He	157	142

Butler & Peterson, PR 129, 836 (1963)
Schwalzchild & Zupancic, PR 129, 854 (1963)

VOLUME 43, NUMBER 20 PHYSICAL REVIEW LETTERS 12 NOVEMBER 1979

Evidence for a Soft Nuclear-Matter Equation of State

Philip J. Siemens[(a)] and Joseph I. Kapusta

Lawrence Berkeley Laboratory, University of California, Berkeley, California 94720

(Received 3 August 1979)

The entropy of the fireball formed in central collisions of heavy nuclei at center-of-mass kinetic energies of a few hundred MeV per nucleon is estimated from the ratio of deuterons to protons at large transverse momentum. The observed paucity of deuterons suggests that strong attractive forces are present in hot, dense nuclear matter, or that degrees of freedom beyond the nucleon and pion may already be realized at an excitation energy of 100 MeV per baryon.

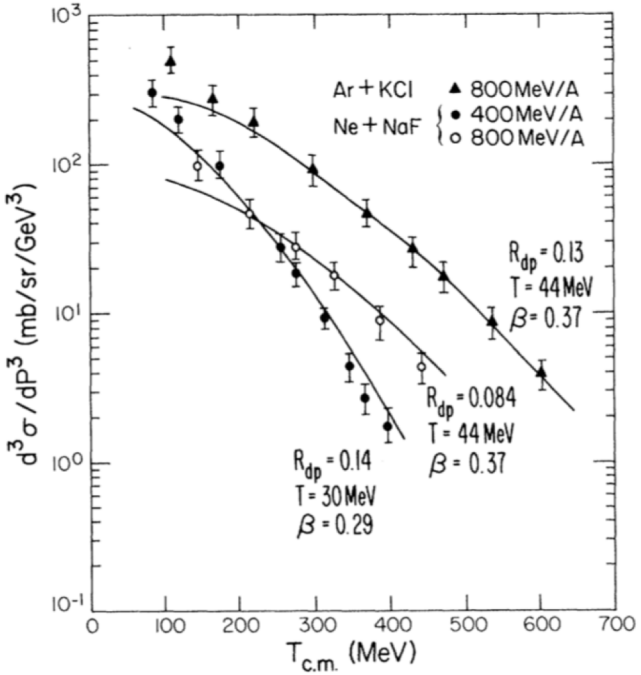

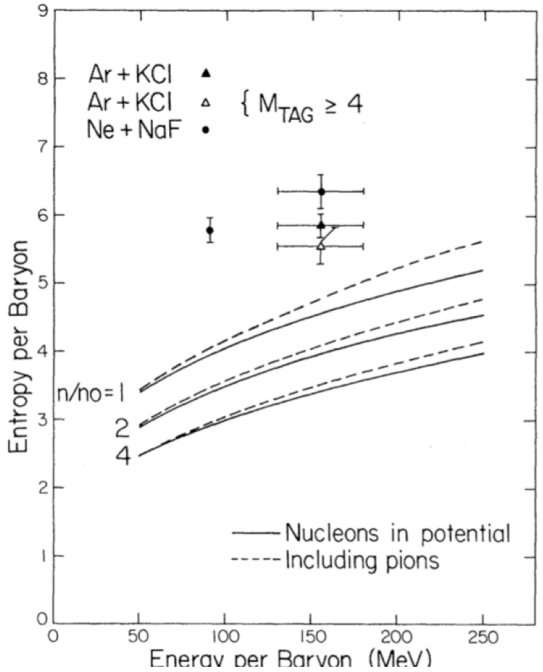

Entropy per baryon and the d/p ratio

Siemens & Kapusta, PRL 43, 1486 (1979)

$$\frac{S}{N} = \frac{E}{T} + \ln Z = \frac{3}{2}N + \ln\frac{(4V/\lambda_{\rm th}^3)^N}{N!}, \qquad \lambda_{\rm th} = \left(\frac{2\pi}{mT}\right)^{1/2}$$

$$\approx N\ln\left[\frac{(4V/N)}{\lambda_{\rm th}^3}e^{5/2}\right], \qquad \ln N! \approx N\ln N - N = N\ln(N/e)$$

$$= \frac{5}{2} - \ln\left[\frac{N}{4V}\lambda_{\rm th}^3\right]$$

Since $$R_{\rm dp} \equiv \frac{N_{\rm d}}{N_{\rm p}} = \frac{3V\gamma_{\rm n}\gamma_{\rm p}2^{3/2}/\lambda_{\rm th}^3}{2V\gamma_{\rm p}/\lambda_{\rm th}^3} = 3\sqrt{2}\gamma_{\rm n}$$

$$= 3\sqrt{2}\left(\frac{N_{\rm n}}{2V}\right)\lambda_{\rm th}^3 = 3\sqrt{2}\left(\frac{N}{4V}\right)\lambda_{\rm th}^3, \qquad N = 2N_{\rm n}$$

so $$\frac{S}{N} = \frac{5}{2} - \ln\left[\frac{N}{4V}\lambda_{\rm th}^3\right] = \frac{5}{2} - \ln\left(\frac{R_{\rm dp}}{3\sqrt{2}}\right)$$

$$= \frac{5}{2} + \ln(3\sqrt{2}) - \ln R_{\rm dp} \approx 3.95 - \ln R_{\rm dp}$$

Coalescence production of light nuclei at AGS

Kahana et al., PRC 54, 388 (1996)

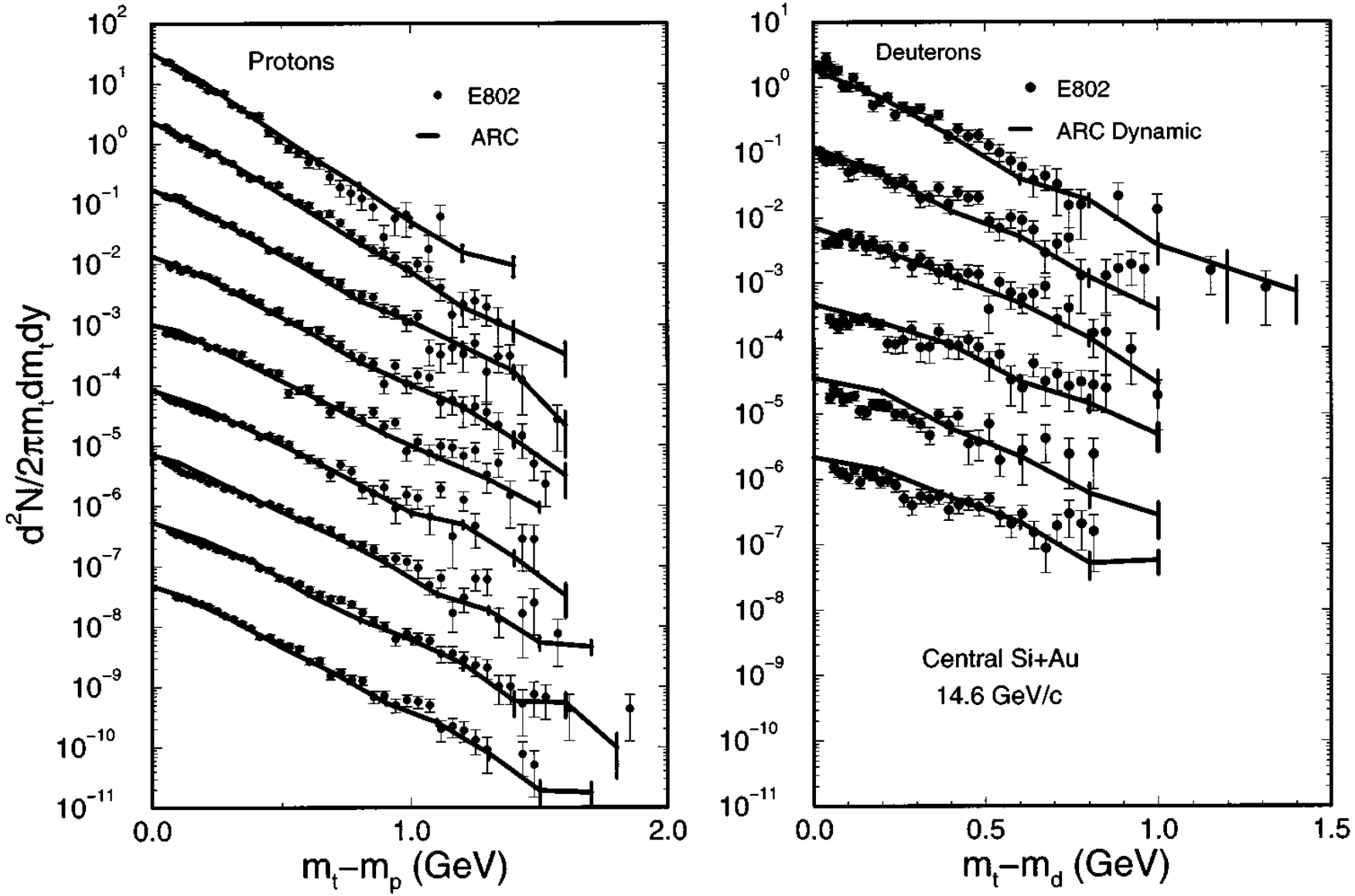

Binding energy effect on light nuclei production

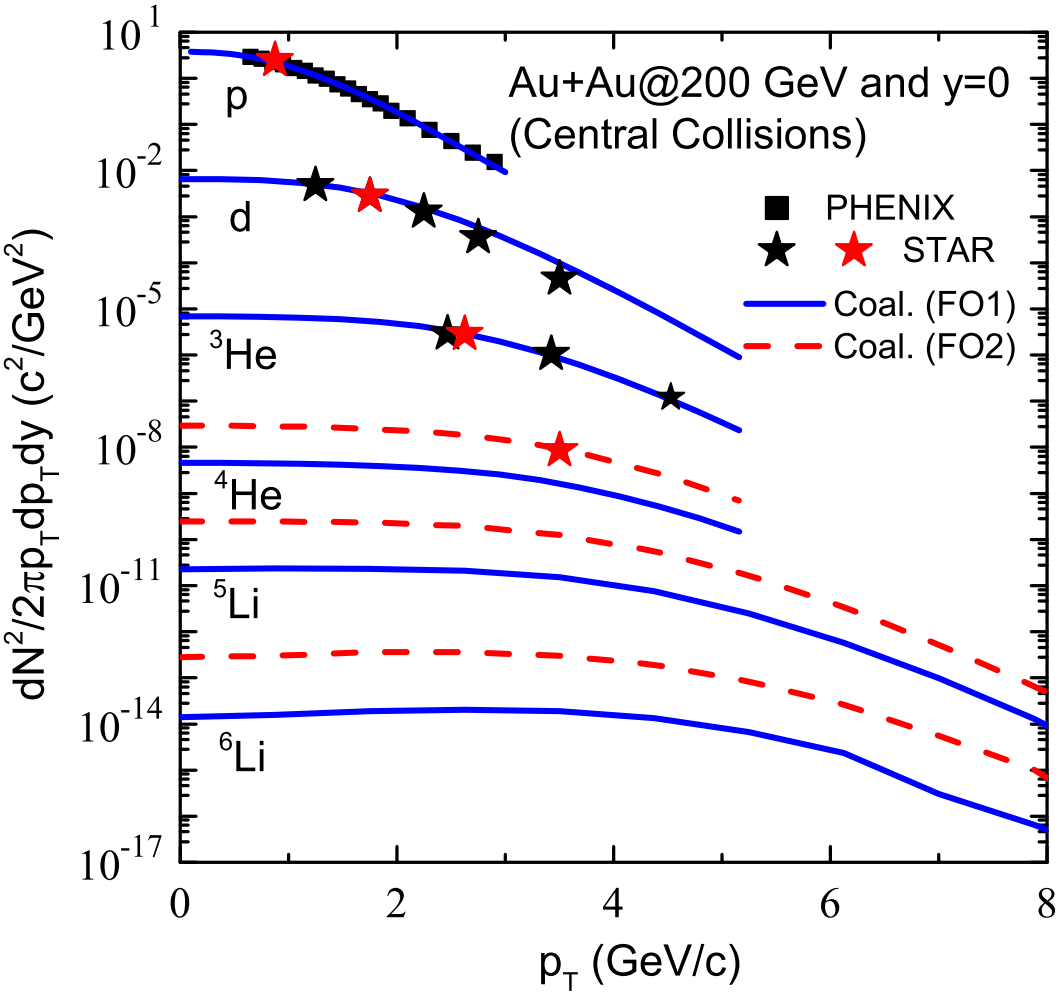

Sun and Chen, PLB 751, 272 (2015)

- ^{4}He is formed earlier because its larger binding energy.
- Assuming a similar effect for ^{5}Li and ^{6}Li leads to their enhanced production.

Table 1

Parameters of the blast-wave-like analytical parametrization for (anti-)nucleon phase–space freezeout configuration.

	T (MeV)	ρ_0	R_0 (fm)	τ_0 (fm/c)	$\Delta\tau$ (fm/c)	ξ_p	$\xi_{\overline{p}}$
FO1	111.6	0.98	15.6	10.55	3.5	10.45	7.84
FO2	111.6	0.98	12.3	8.3	3.5	21.4	16.04

Extended blast-wave model for light nuclei production

Yin, ko, Sun & Zhu, PRC 95, 054913 (2017)

$$\text{Momentum} - \text{space correlation} : R = R_0 e^{a(p_T - p_0)}, \ (|p_x| > |p_y|)$$

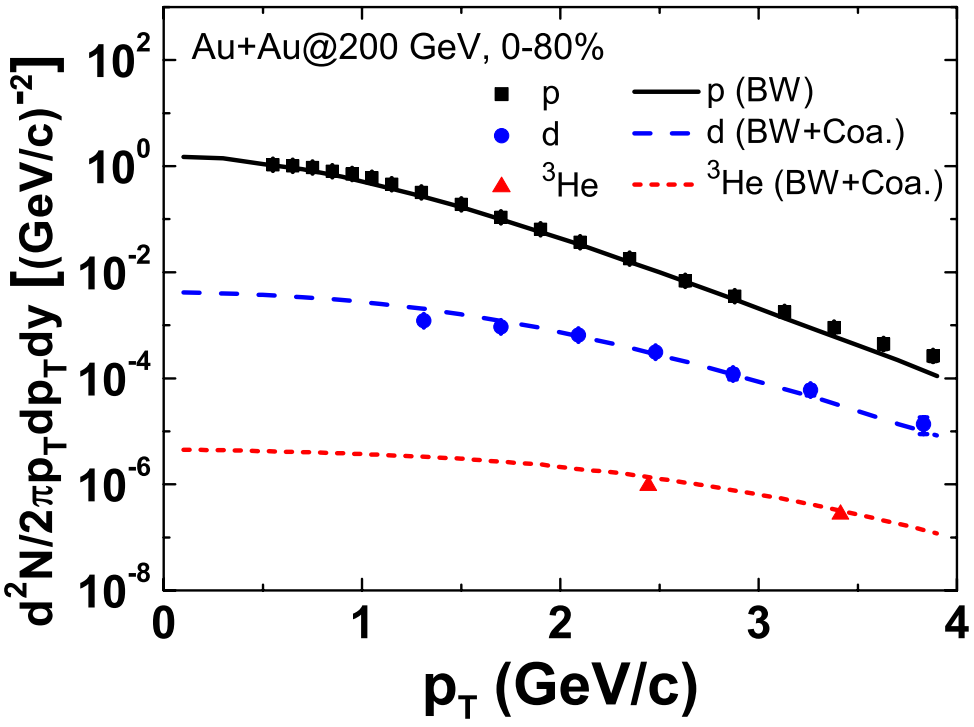

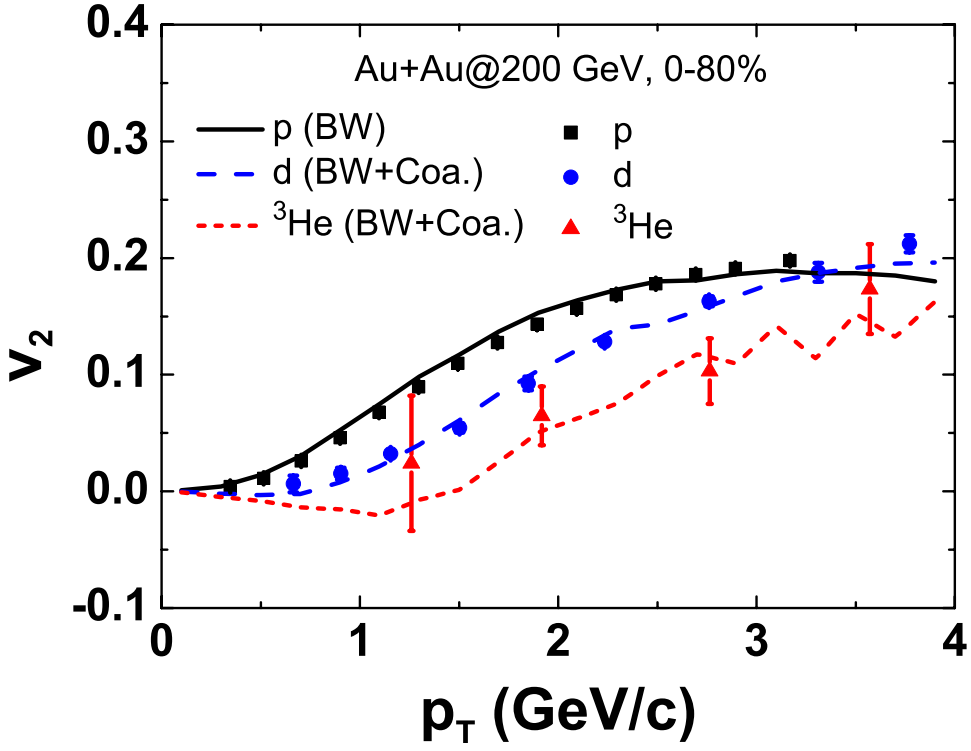

- Both deuteron and ^{3}He elliptic flows are better described after allowing nucleons with momenta larger than p_0=0.9 GeV more spread in space when their momenta are more aligned along the reaction plane.

Ellitpic flow from STAR Beam Energy Scan PRC 94, 034908 (2016)

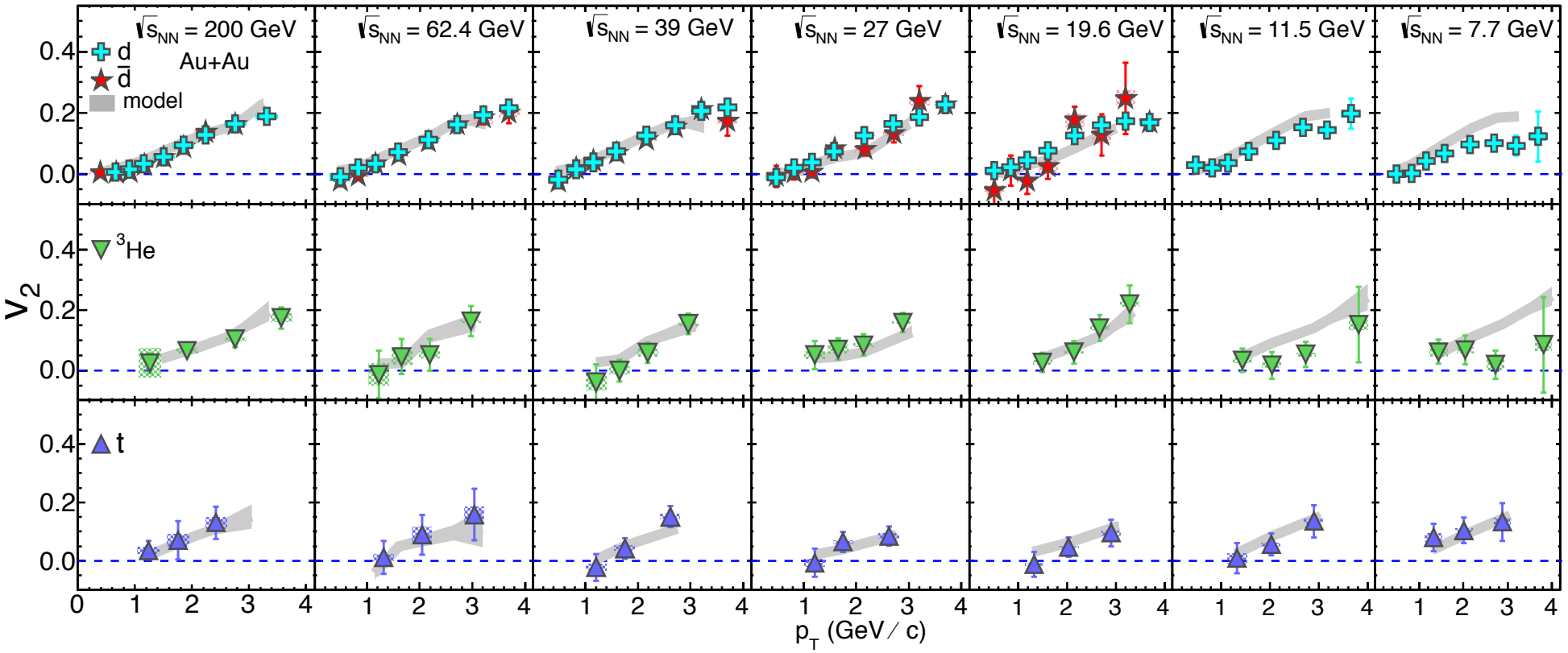

- AMPT + Coalescence reproduces data reasonably well.
- Blast wave mode fails.

PHYSICAL REVIEW C **98**, 054905 (2018)

Spectra and flow of light nuclei in relativistic heavy ion collisions at energies available at the BNL Relativistic Heavy Ion Collider and at the CERN Large Hadron Collider

Wenbin Zhao,[1,2] Lilin Zhu,[3] Hua Zheng,[4,5] Che Ming Ko,[6] and Huichao Song[1,2,7]

IEBE-VISHNU hybrid model with AMPT initial conditions

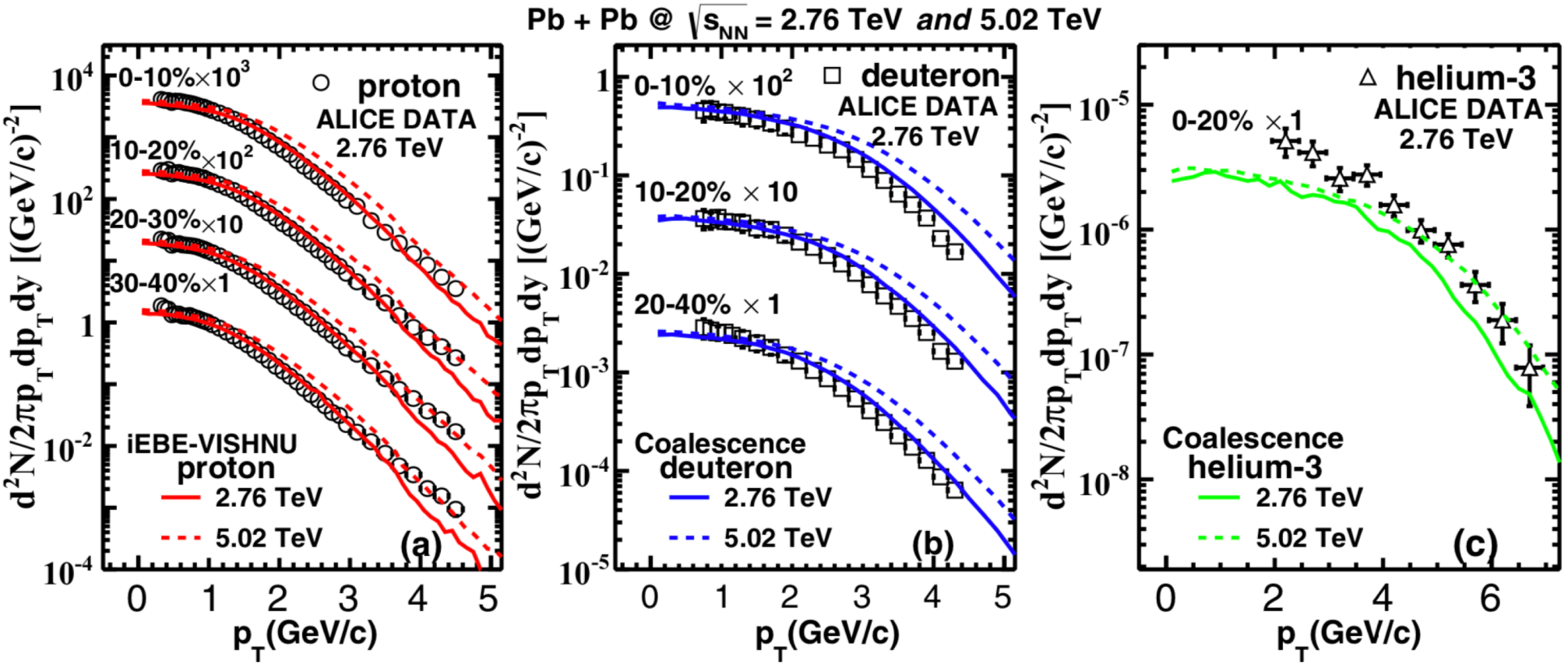

Elliptic flow of deuteron measured by ALICE is also satisfactorily described.

Particle yields in thermal model

Braun-Munzinger and Donigus, NPA 987, 144 (2019)

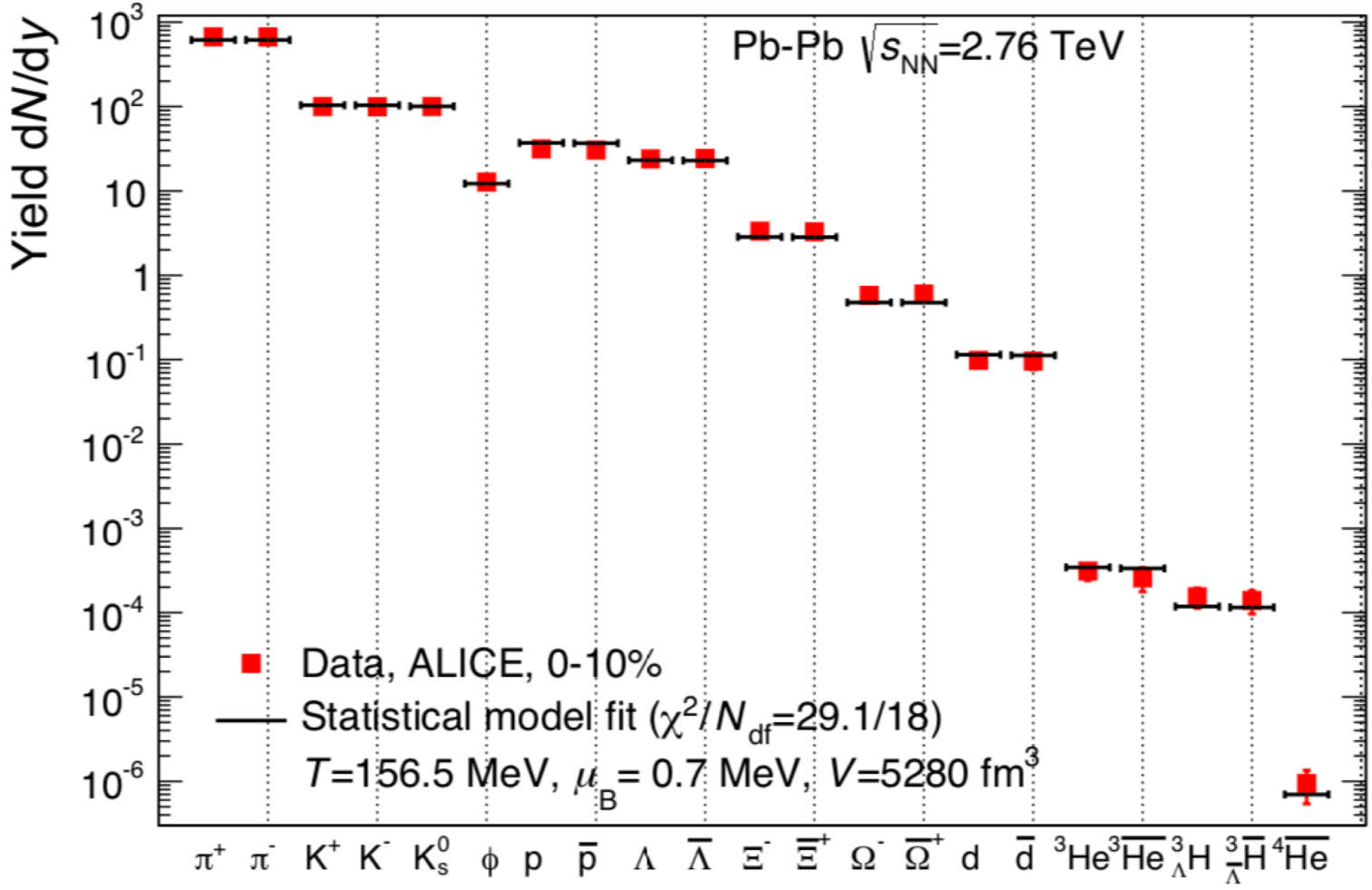

Figure 11: Thermal model description of the production yields (rapidity density) of different particle species in heavy-ion collisions at the LHC for a chemical freeze-out temperature of 156.5 MeV (from [59], where more details can be found, see also [60]).

Coalescence model in the sudden approximation

Wave functions for initial |i>=|1,2> and final |f>=|3> states

$$\langle \mathbf{r}_1, \mathbf{r}_2 | i \rangle = \phi_1(\mathbf{r}_1)\phi_2(\mathbf{r}_2)$$

$$\langle \mathbf{r}_1, \mathbf{r}_2 | f \rangle = \frac{1}{\sqrt{V}} e^{i\mathbf{K}\cdot(\mathbf{r}_1+\mathbf{r}_2)/2} \Phi(\mathbf{r}_1 - \mathbf{r}_2)$$

Probability for 1+2 -> 3

$$\mathcal{P} = |\langle f | i \rangle|^2$$

Probability for particle 1 of momentum $\mathbf{k}_1$ and particle 2 of momentum $\mathbf{k}_2$ to coalescence to cluster 3 with momentum **K**

$$\frac{dN}{d^3\mathbf{K}} = g \int d^3\mathbf{x}_1 d^3\mathbf{k}_1 d^3\mathbf{x}_2 d^3\mathbf{k}_2 W_1(\mathbf{x}_1, \mathbf{k}_1) W_2(\mathbf{x}_2, \mathbf{k}_2)$$

$$\times W(\mathbf{y}, \mathbf{k}) \delta^{(3)}(\mathbf{K} - \mathbf{k}_1 - \mathbf{k}_2), \qquad \mathbf{y} = \mathbf{x}_1 - \mathbf{x}_2, \quad \mathbf{k} = \frac{\mathbf{k}_1 - \mathbf{k}_2}{2}$$

Wigner functions $W(\mathbf{x}, \mathbf{k}) = \int d^3\mathbf{y} \phi^* \left(\mathbf{x} - \frac{\mathbf{y}}{2}\right) \phi \left(\mathbf{x} + \frac{\mathbf{y}}{2}\right) e^{-i\mathbf{k}\cdot\mathbf{y}}$

For a system of particles 1 and 2 with phase-space distributions $f_i(\mathbf{x}_i,\mathbf{k}_i)$ normalized to $\int d^3\mathbf{x_i}d^3\mathbf{k}_i f_i(\mathbf{x}_i,\mathbf{k}_i) = N_i$, the number of particle 3 produced from coalescence of N_1 of particle 1 and N_2 of particle 2

$$\begin{aligned}\frac{dN}{d^3\mathbf{K}} &\approx g\int d^3\mathbf{x}_1 d^3\mathbf{k}_1 d^3\mathbf{x}_2 d^3\mathbf{k}_2 f_1(\mathbf{x}_1,\mathbf{k}_1) f_2(\mathbf{x}_2,\mathbf{k}_2) \\ &\times \overline{W}(\mathbf{y},\mathbf{k})\delta^{(3)}(\mathbf{K}-\mathbf{k}_1-\mathbf{k}_2)\end{aligned}$$

$$\overline{W}(\mathbf{y},\mathbf{k}) = \int \frac{d^3\mathbf{x}_1' d^3\mathbf{k}_1'}{(2\pi)^3}\frac{d^3\mathbf{x}_2' d^3\mathbf{k}_2'}{(2\pi)^3} W_1(\mathbf{x}_1',\mathbf{k}_1') W_2(\mathbf{x}_2',\mathbf{k}_2') W(\mathbf{y}',\mathbf{k}')$$

Wigner function $W_i(\mathbf{x}_i',\mathbf{k}_i')$ centers around $\mathbf{x}_i$ and $\mathbf{k}_i$

$g = \frac{2J+1}{(2J_1+1)(2J_2+1)}$ Statistical factor for two particles of spin J_1 and J_2 to form a particle of spin J

The above formula can be straightforwardly generalized to multi-particle coalescence, but is usually used by taking particle Wigner functions as delta functions in space and momentum.

Gyulassy, Frankel, and Remler, NPA 402, 596 (1983): Generalized coalescence model using nucleon Wigner functions that are delta functions in space and momentum, i.e., evaluating

$$\overline{W}(\mathbf{y},\mathbf{k}) = \int \frac{d^3\mathbf{x}_1' d^3\mathbf{k}_1'}{(2\pi)^3} \frac{d^3\mathbf{x}_2' d^3\mathbf{k}_2'}{(2\pi)^3} W_1(\mathbf{x}_1',\mathbf{k}_1') W_2(\mathbf{x}_2',\mathbf{k}_2') W(\mathbf{y}',\mathbf{k}')$$

with $W_i(\mathbf{x}_i',\mathbf{k}_i') = (2\pi)^3 \delta^3(\mathbf{x}_i' - \mathbf{x}_i)\delta^3(\mathbf{k}_i' - \mathbf{k}_i)$

$$\begin{aligned} \rightarrow \frac{dN}{d^3\mathbf{K}} &\approx g \int d^3\mathbf{x}_1 d^3\mathbf{k}_1 d^3\mathbf{x}_2 d^3\mathbf{k}_2 f_1(\mathbf{x}_1,\mathbf{k}_1) f_2(\mathbf{x}_2,\mathbf{k}_2) \\ &\times W(\mathbf{y},\mathbf{k}) \delta^{(3)}(\mathbf{K} - \mathbf{k}_1 - \mathbf{k}_2) \end{aligned}$$

It is later called by Kahana et al. the standard Wigner calculation in contrast to the general one which they called the quantum Wigner calculation.

Deuteron number in the coalescence model

In the coalescence model, the deuteron number is given by

$$N_d = g_d \int d^3\mathbf{x}_1 \int d^3\mathbf{k}_1 \int d^3\mathbf{x}_2 \int d^3\mathbf{k}_2 f_1(\mathbf{x}_1, \mathbf{k}_1) f_2(\mathbf{x}_2, \mathbf{k}_2) W_d(\mathbf{x}_1 - \mathbf{x}_2, (\mathbf{k}_1 - \mathbf{k}_2)/2).$$

In the above, the proton or neutron distribution function is given by

$$f(\mathbf{x}, \mathbf{k}) = \frac{2\gamma}{(2\pi)^3}\, e^{-\frac{k^2}{2mT}},$$

where T, m and γ are the temperature, nucleon mass, and fugacity, respectively, and is normalized to

$$N = \int d^3\mathbf{x} \int d^3\mathbf{k} f(\mathbf{x}, \mathbf{k}) = 2\gamma V \left(\frac{mT}{2\pi}\right)^{3/2}.$$

after using

$$\int d^3\mathbf{x} = V, \quad \int d^3\mathbf{k}\, e^{-ak^2} = \left(\frac{\pi}{a}\right)^{3/2},$$

with V being the volume. The deuteron Wigner function is given by

$$W_d(\mathbf{x}, \mathbf{k}) = 8\, e^{-\frac{x^2}{\sigma^2}}\, e^{-\sigma^2 k^2},$$

and is normalized according to

$$\int d^3\mathbf{x} \int d^3\mathbf{k}\, W_d(\mathbf{x}, \mathbf{k}) = (2\pi)^3.$$

Deuteron number in the coalescence model (Continued)

Changing variables to

$$\begin{aligned} \mathbf{X} &= \frac{\mathbf{x}_1 + \mathbf{x}_2}{2}, \quad \mathbf{x} = \mathbf{x}_1 - \mathbf{x}_2, \\ \mathbf{K} &= \mathbf{k}_1 + \mathbf{k}_2, \quad \mathbf{k} = \frac{\mathbf{k}_1 - \mathbf{k}_2}{2}, \end{aligned}$$

then

$$\begin{aligned} N_d &= \frac{32 g_d \gamma_1 \gamma_2}{(2\pi)^6} \int d^3\mathbf{X} \int d^3\mathbf{x}\; e^{-\frac{x^2}{\sigma^2}} \int d^3\mathbf{K}\; e^{-\frac{K^2}{4mT}} \int d^3\mathbf{k}\; e^{-k^2(\sigma^2 + \frac{1}{mT})} \\ &= \frac{32 g_d \gamma_1 \gamma_2}{(2\pi)^6}\, V\, (\pi\sigma^2)^{3/2}\, (4\pi m T)^{3/2} \left(\frac{\pi}{\sigma^2 + \frac{1}{mT}}\right)^{3/2} \\ &= 2^{3/2} g_d \left(\frac{2\pi}{mT + \frac{1}{\sigma^2}}\right)^{3/2} \frac{N_1 N_2}{V} \\ &= \frac{3}{2^{1/2}} \left(\frac{2\pi}{mT}\right)^{3/2} \frac{1}{\left(1 + \frac{1}{mT\sigma^2}\right)^{3/2}} \frac{N_1 N_2}{V}, \quad (g_d = 3/4) \\ &\approx \frac{3}{2^{1/2}} \left(\frac{2\pi}{mT}\right)^{3/2} \frac{N_1 N_2}{V}, \quad (mT \gg 1/\sigma^2) \end{aligned}$$

In this limit, the coalescence model gives

$$N_{\rm d}^{\rm coal} \approx \frac{3}{2^{1/2}}\left(\frac{2\pi}{mT}\right)^{3/2}\frac{N_1 N_2}{V} = \frac{3}{2^{1/2}}4V\gamma_1\gamma_2\left(\frac{mT}{2\pi}\right)^{3/2}$$

$$= 3V\gamma_1\gamma_2\left(\frac{mT}{\pi}\right)^{3/2}$$

Compared with the thermal model,

$$N_{\rm d}^{\rm thermal} \approx \frac{3V\gamma_1\gamma_2}{(2\pi)^3}\int d^3{\rm k}e^{-\frac{k^2}{4mT}}e^{\frac{B_{\rm d}}{T}}$$

$$= 3V\gamma_1\gamma_2\left(\frac{mT}{\pi}\right)^{3/2}e^{\frac{B_d}{T}}$$

so $N_{\rm d}^{\rm coal} \approx N_{\rm d}^{\rm thermal}$ if $T \gg B_{\rm d}$ and $mT \gg 1/\sigma^2$

Why $N_{\rm d}^{\rm thermal}(T_{\rm C}) = N_{\rm d}^{\rm thermal}(T_{\rm K})$?

Time evolution of baryon entropy in relativistic heavy ion collisions from the hadronic phase of AMPT

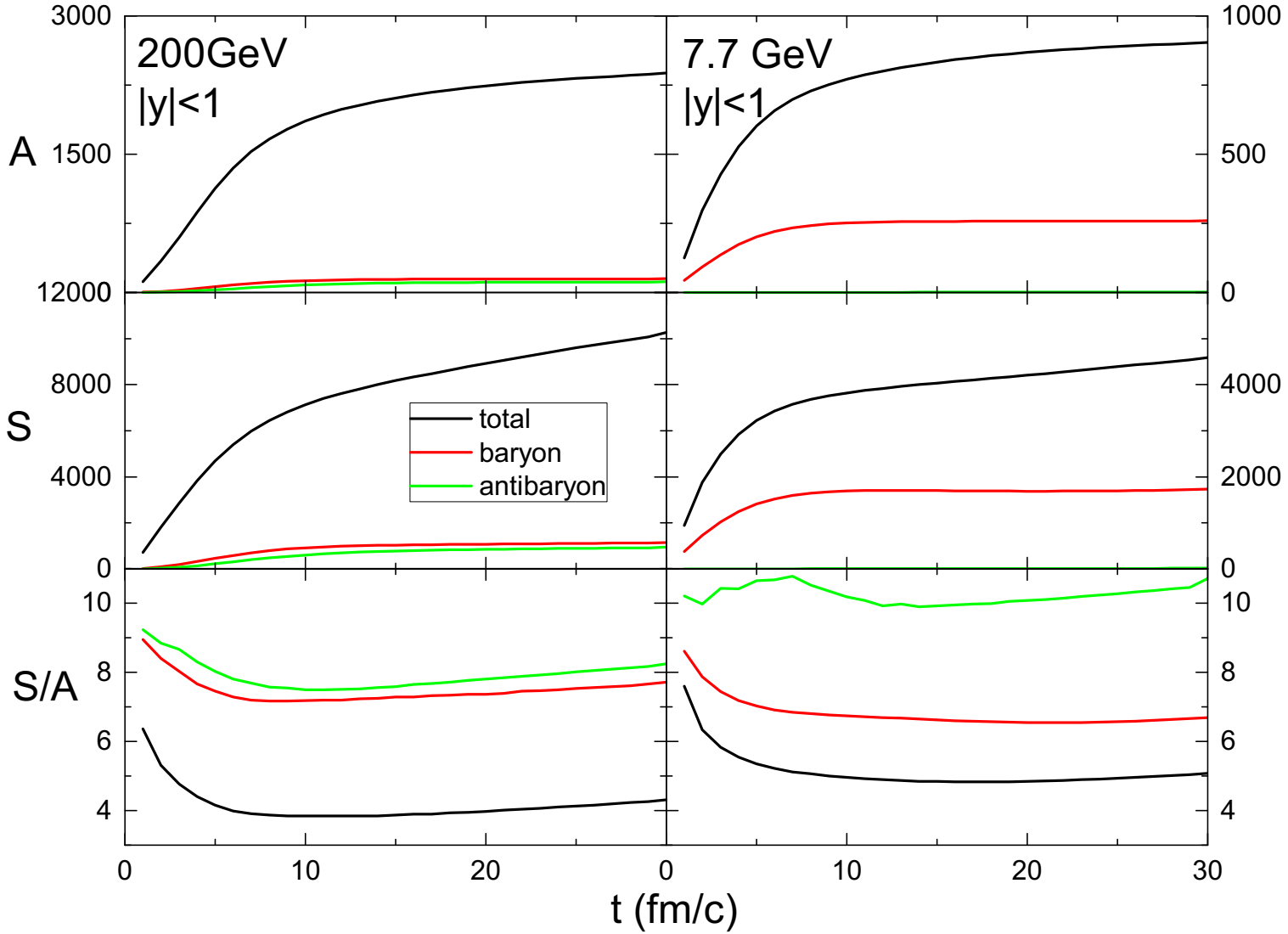

- Baryon entropy per baryon remains essentially constant during hadronic evolution, thus similar d/p ratio at T_C and T_K.

Chemical freeze-out in relativistic heavy ion collisions

Jun Xu & CMK, PLB 772, 290 (2017)

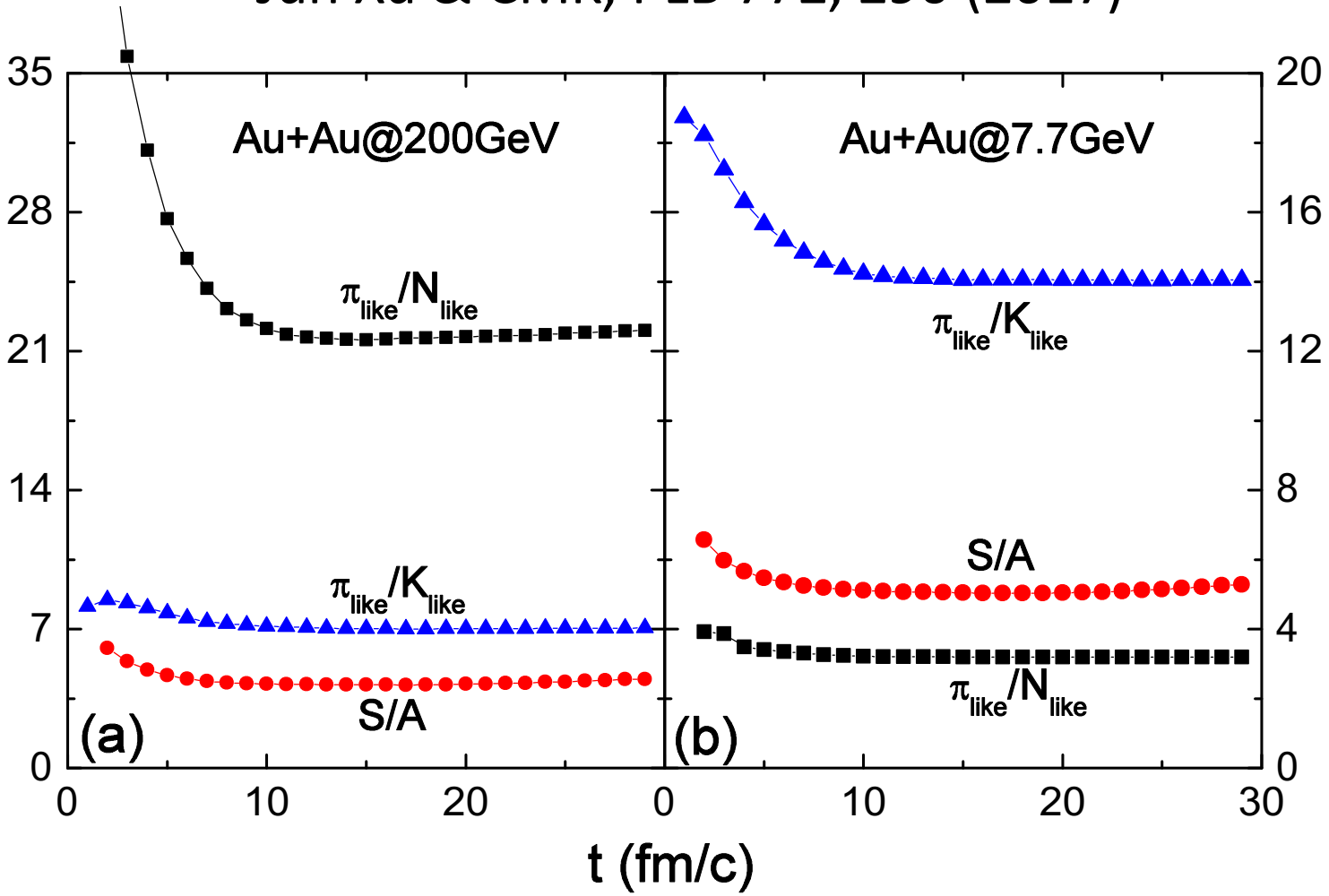

- Both ratio of effective particle numbers and entropy per particle remain essentially constant from chemical to kinetic freeze-out.

Deuteron production from an extended ART model

Oh & Ko, PRC 76, 054910 (2007); Oh, Lin & Ko, PRC 80, 064902 (2009)

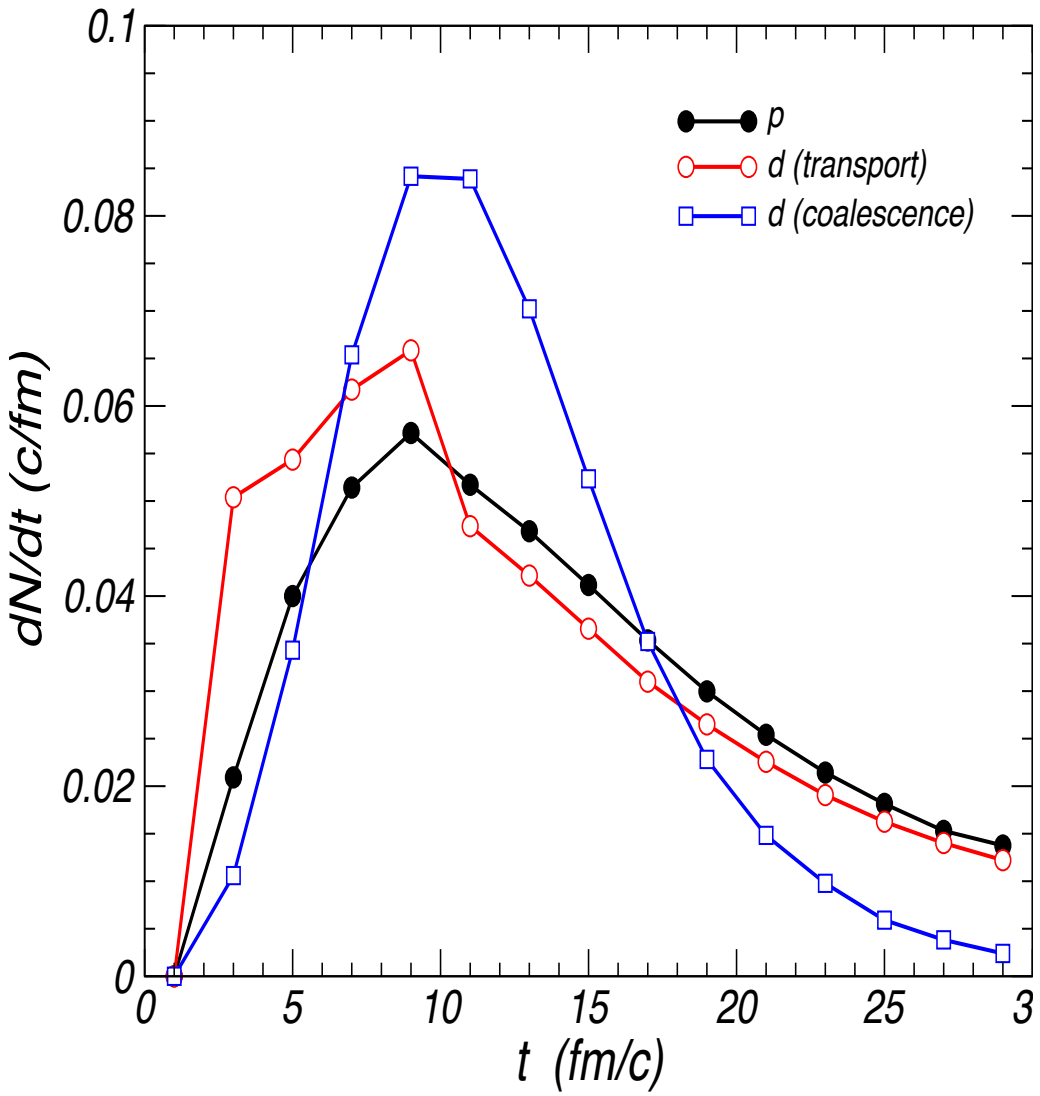

- Include deuteron production ($n+p \rightarrow d+\pi$) and annihilation ($d+\pi \rightarrow n+p$) as well as its elastic scattering
- Similar emission time distributions for protons and deuterons in coalescence model
- Slight different deuteron emission time distribution in transport and coalescence models

Time evolution of proton and deuteron numbers

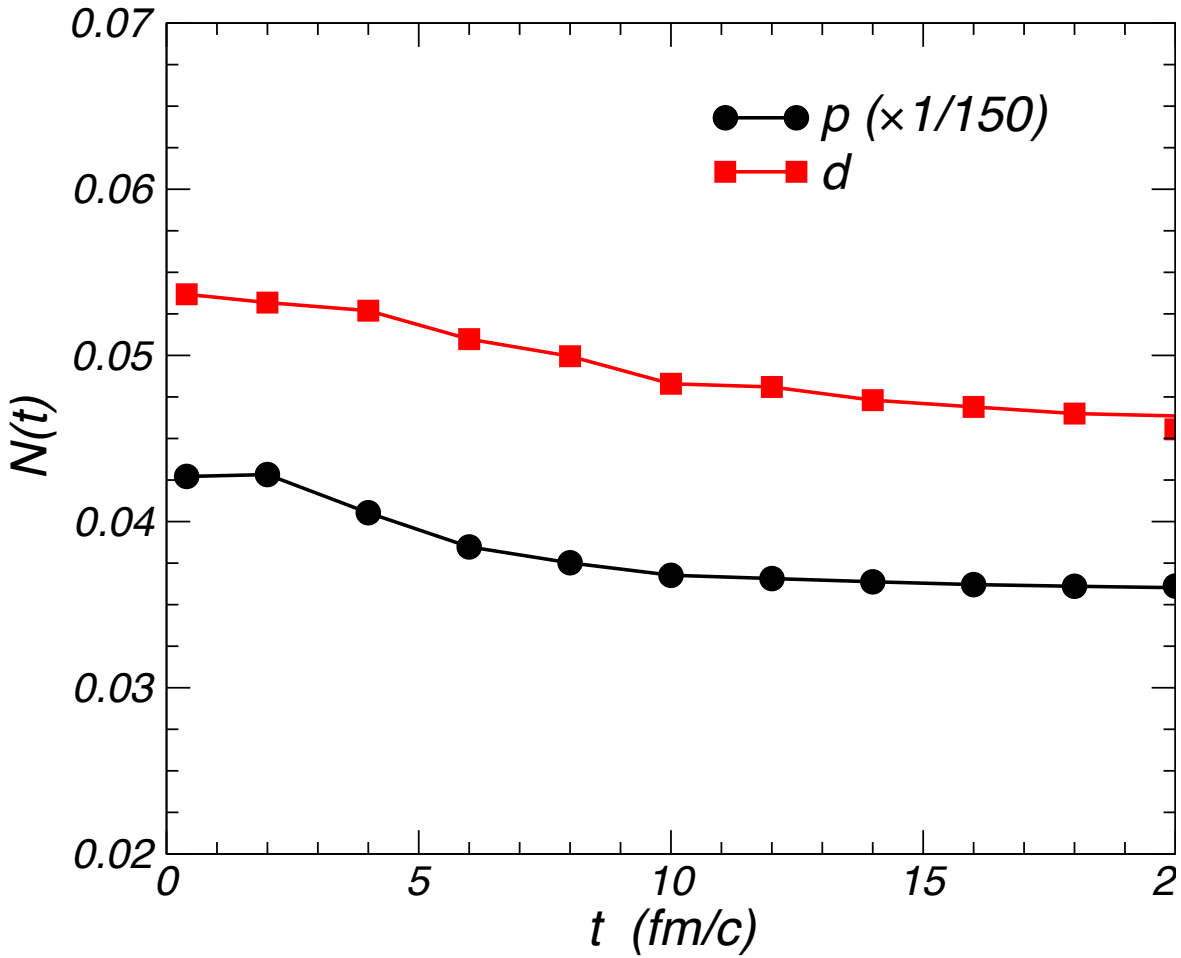

- Both proton and deuteron numbers decrease only slightly with time → early chemical equilibration

Deuteron production in SMASH

Oliinychekov, Pang, Elfner & Koch, PRC 99, 044907 (2019)

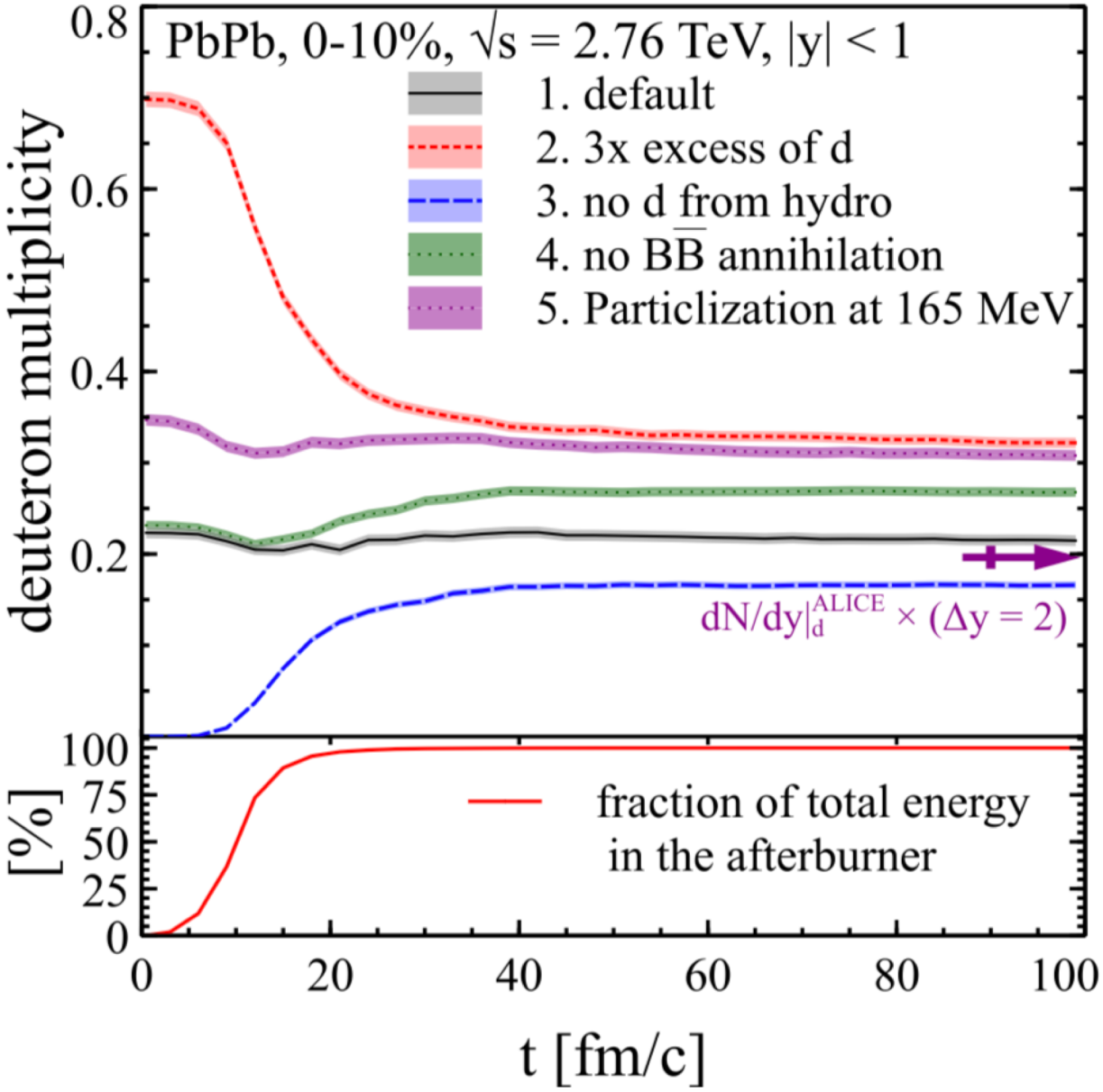

- Using a large $\pi NN \leftrightarrow \pi d$ cross section of about 100 mb.
- Deuteron number essentially remains unchanged during hadronic evolution

Deuteron production in kinetic theory

Cho & Lee, PRC 97, 024911 (2018)

$$\frac{dN_d(\tau)}{d\tau} = \sum_i \langle \sigma_{Ni} v_{Ni} \rangle n_i N_N(\tau) - \sum_i \langle \sigma_{di} v_{di} \rangle n_i N_d(\tau)$$

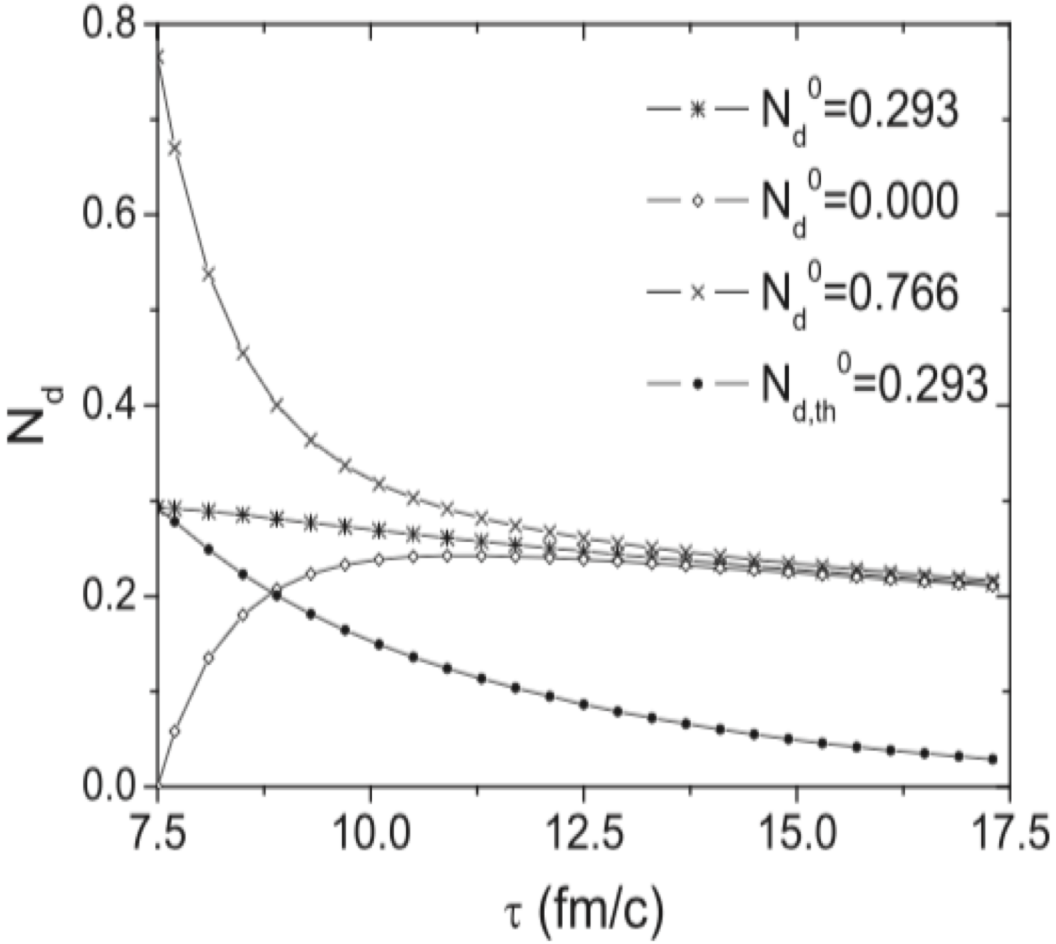

- Using

  $\sigma(d\pi^+ \to pp) = 50$ mb

  to take into account the large cross section due to $d\pi^+ \to pn\pi^+$
- Time evolution of temperature and volume from a schematic hydro model.
- Final abundance independent of initial abundance.

Binding energies of light nuclei in hot dense matter

G. Roepke

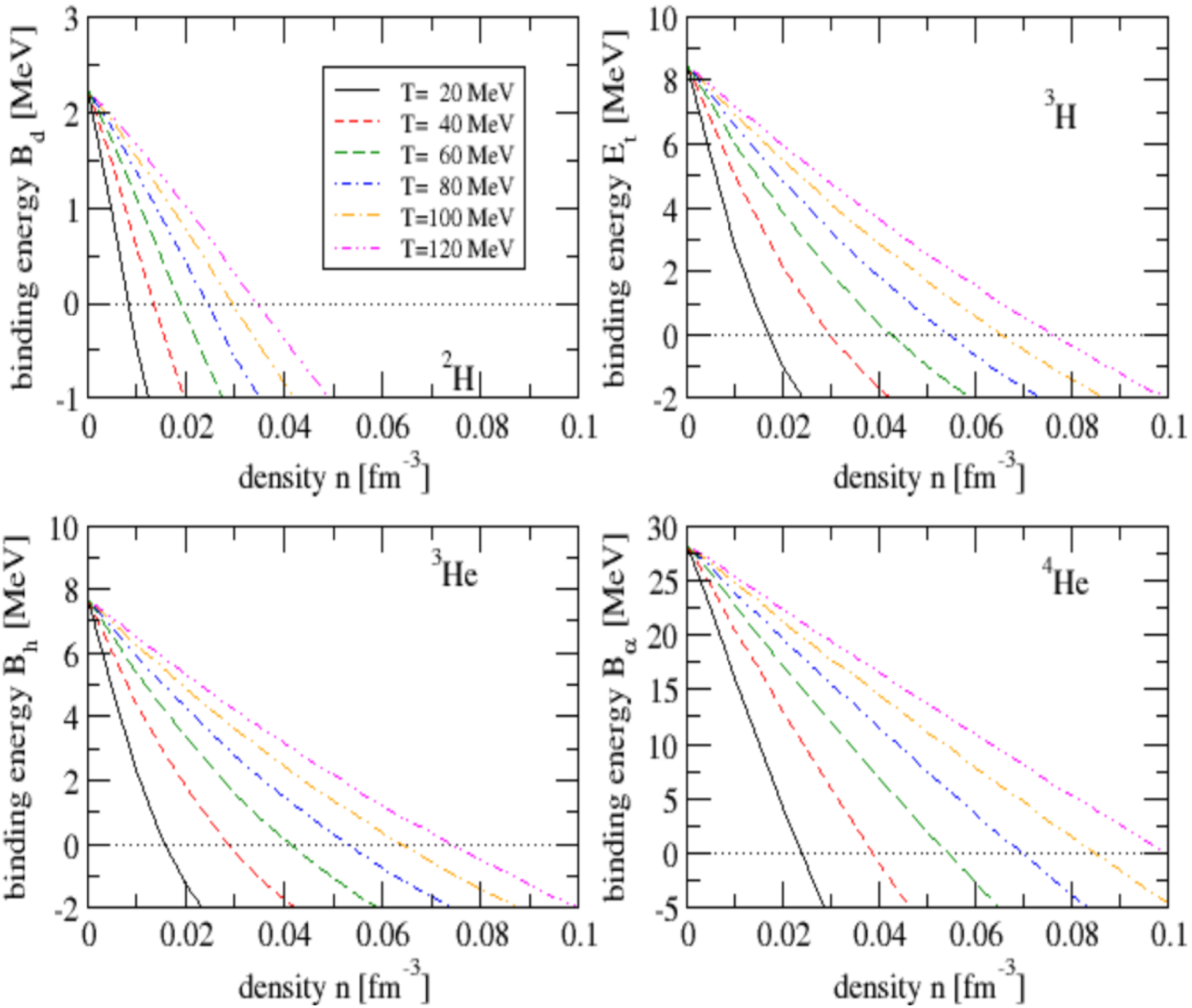

System size dependence of light nuclei yield

Sun, Ko & Doenigus, PLB 792, 132 (2019)

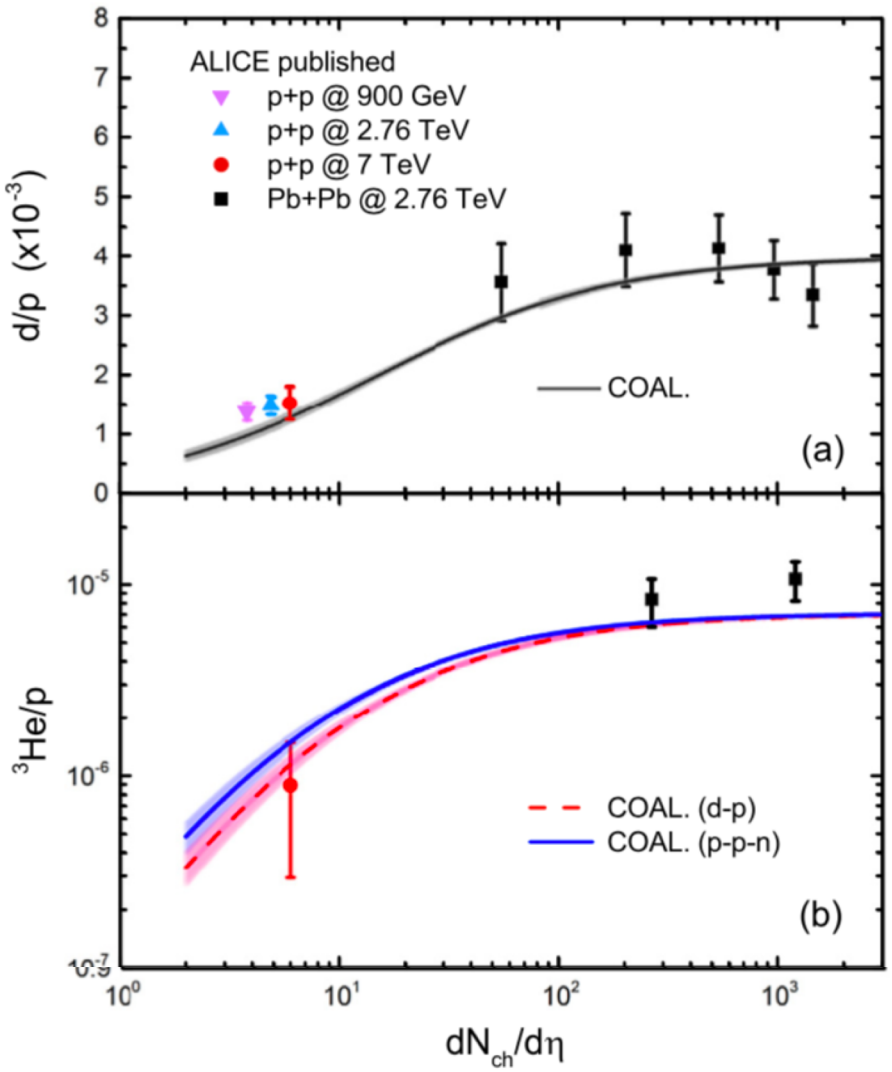

$$\frac{N_d}{N_p} \approx \frac{3N_n}{4(mT_K R^2)^{3/2}} \frac{1}{1+\frac{2r_d^2}{3R^2}}$$

$$\frac{N_{^3He}}{N_p} \approx \frac{N_n N_p}{4(mT_K R^2)^{3/2}} \frac{1}{1+\frac{r_{^3He}^2}{2R^2}}$$

- Coalescence model gives a natural explanation for the suppressed production of light nuclei in small collision systems.
- Thermal model requires an unrealistically large canonical correlation volume for charge conservation. [Vovchenko, Doenigus & Stoecker, PLB 785, 171 (2018)]

Hypertriton production in coalescence model

Zhang & Ko, PLB 780, 191 (2018)

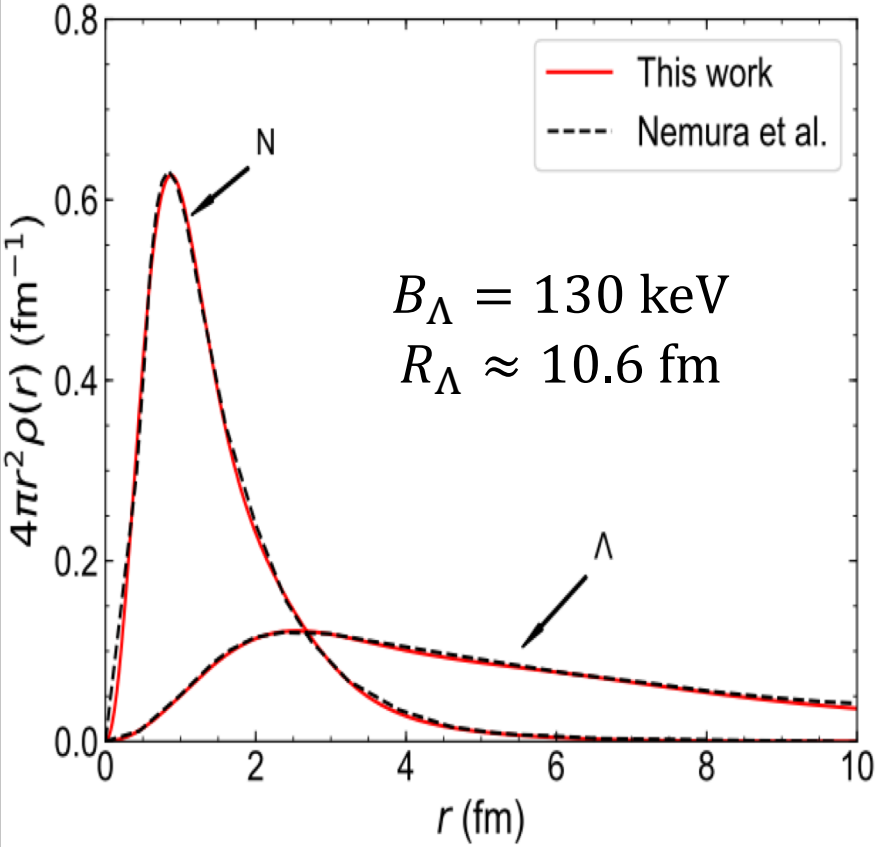

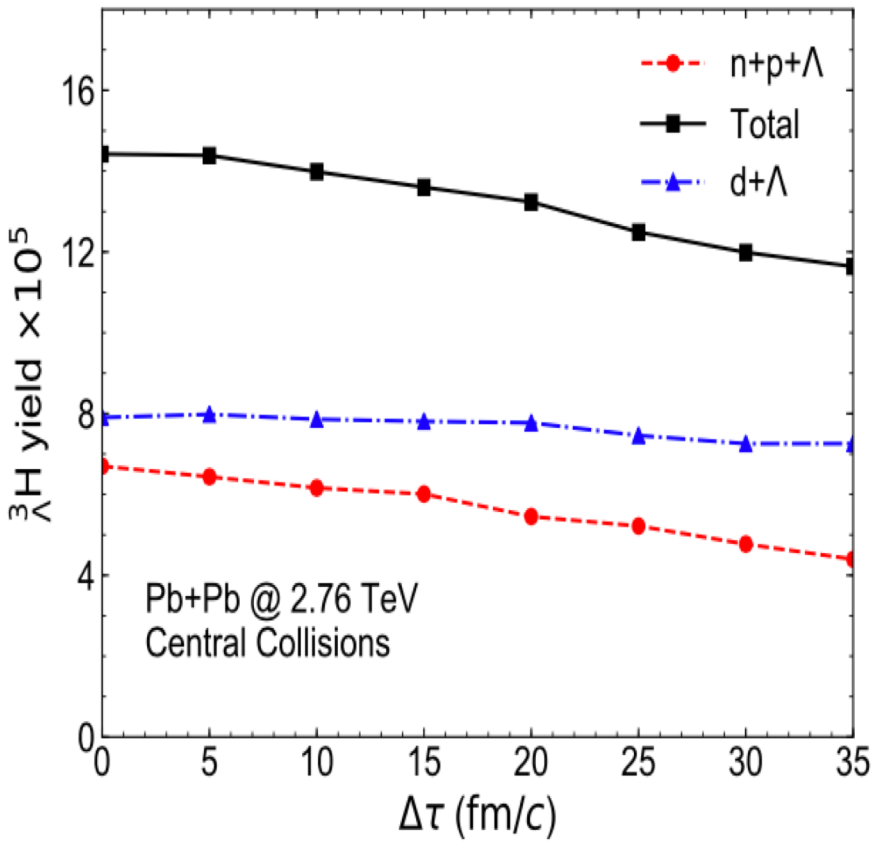

- Because of its large size, hypertriton yield changes little after long free streaming of kinetic freeze out nucleons if produced from their coalescence.

Neutron relative density fluctuation from yield ratio of light nuclei

Sun, Chen, Ko & Xu, PLB 774, 103 (2017); 781, 499 (2018)

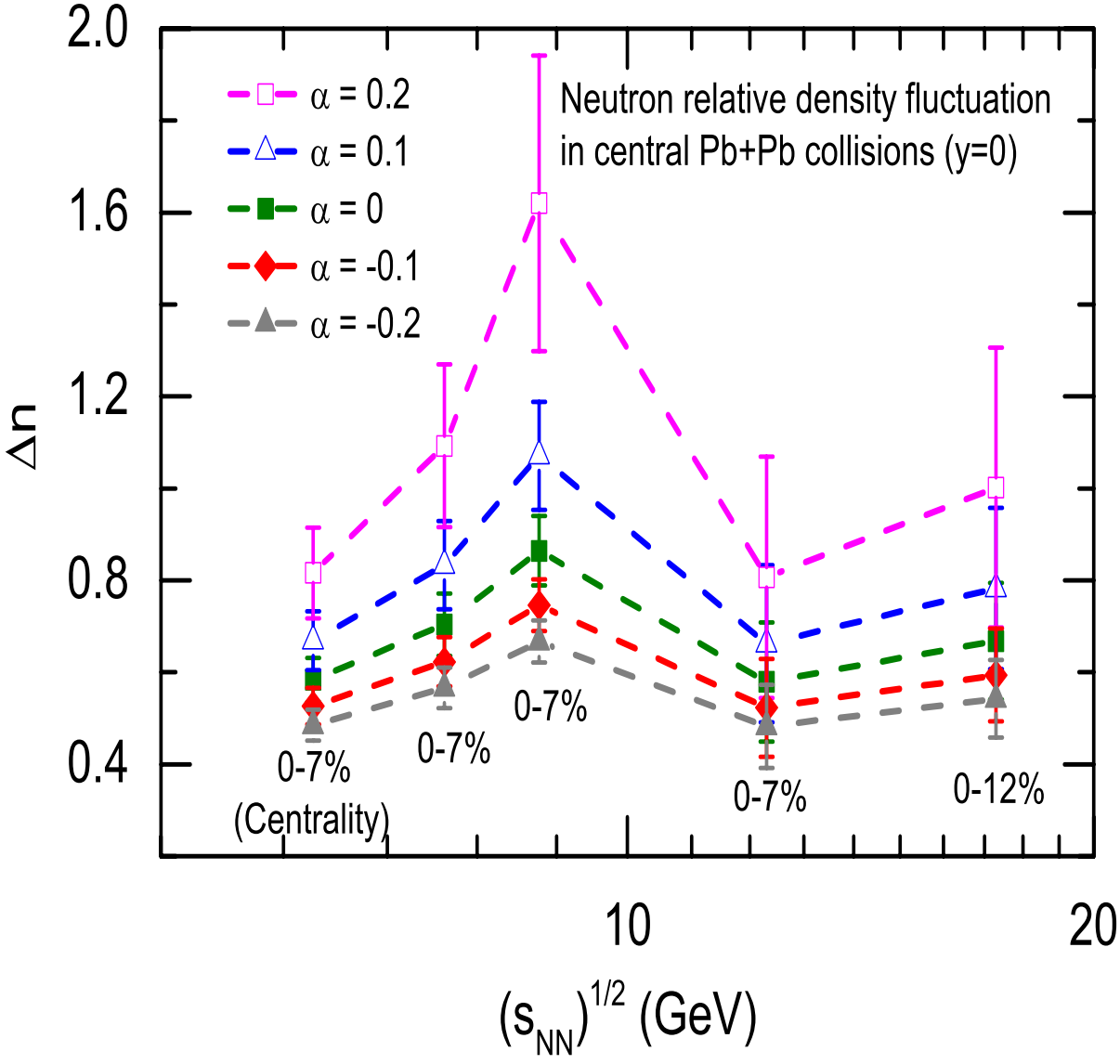

$$\mathcal{O}_{\text{p-d-t}} = \frac{N_{^3\text{H}} N_p}{N_{\text{d}}^2}$$

$$= g\frac{1+(1+2\alpha)\Delta n}{(1+\alpha\Delta n)^2}$$

$$\Delta n = \frac{\langle(\delta n)^2\rangle}{\langle n\rangle^2}$$

$$\langle \delta n \delta n_p \rangle = \alpha \frac{\langle n_p \rangle}{\langle n \rangle}\langle(\delta n)^2\rangle$$

α: correlation factor

$T_C \approx 144$ MeV

$\mu_C \approx 385$ MeV

- Expect a similar behavior for $\frac{pK^0}{\pi^+\Lambda}$ from u-quark density fluctuation.

Neutron relative density fluctuation from STAR data

Dingwei Zhang, for the STAR Collaboration, QM2018

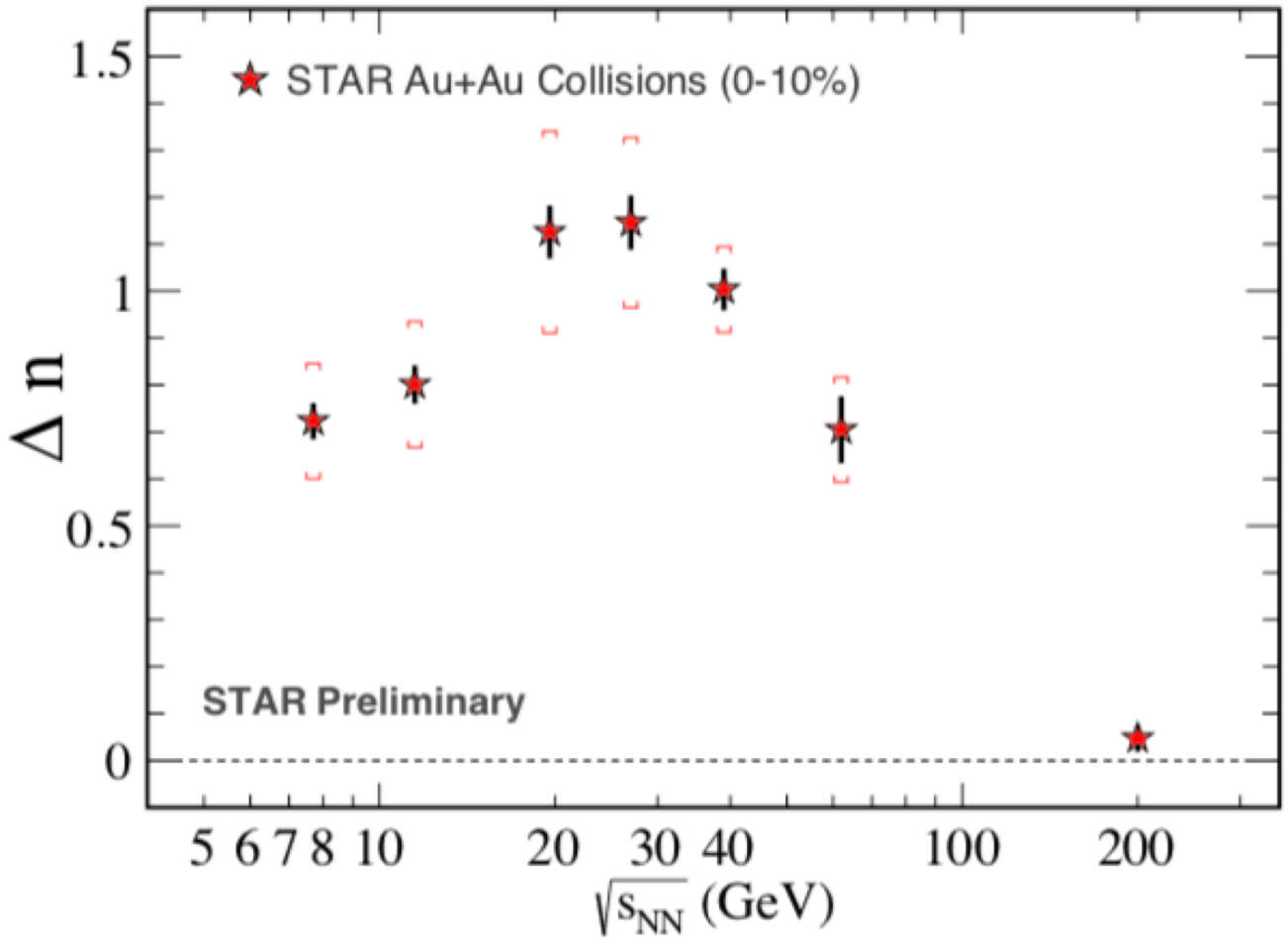

- Neutron density fluctuation extracted from $N_t N_p / N_d^2$ also shows a peak like at SPS but at a higher energy.

Transport description of quark matter in a box based on NJL

$$\partial_t f + \mathbf{p}/E \cdot \nabla f - \nabla H \cdot \nabla_p f = \mathcal{C}[f]$$ Feng & Ko, PRC 93, 035205 (16); 95, 055203 (17)

C[f] includes quark elastic scattering with cross section of 3 mb

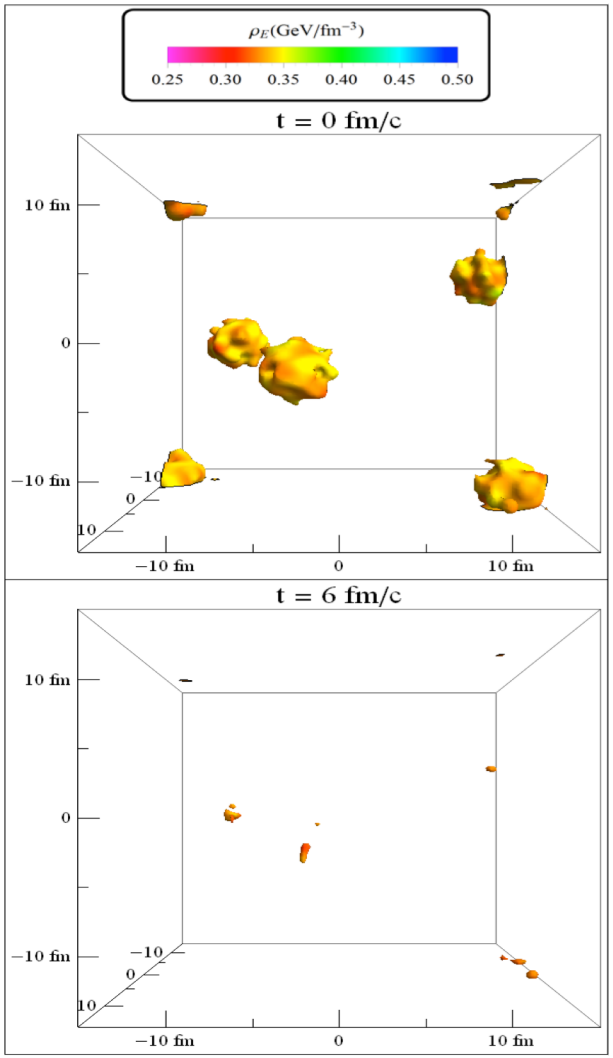

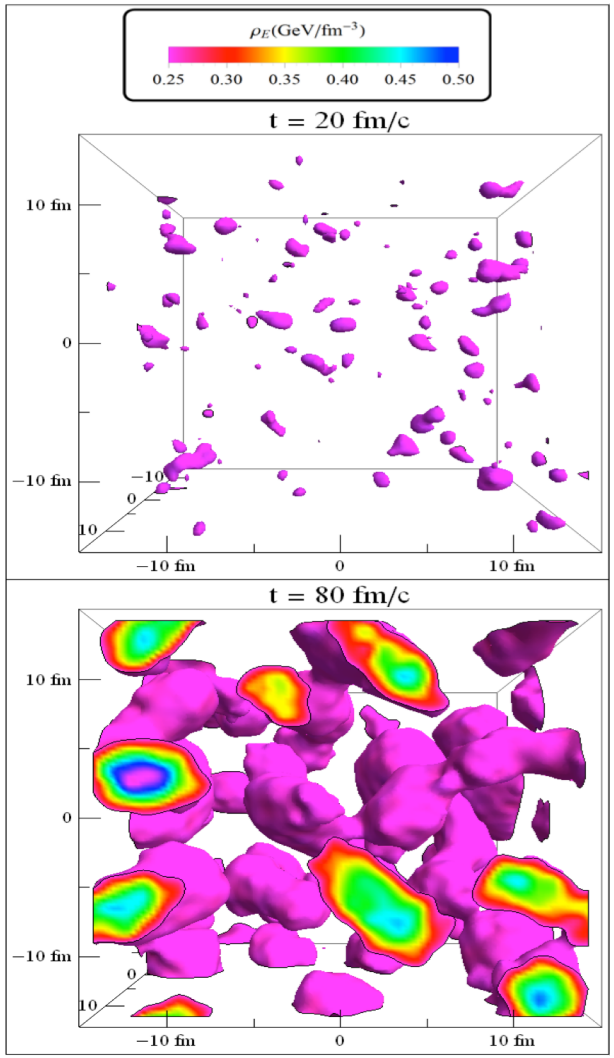

- Left: n_q = 0.4/fm^3, T = 100 MeV; outside spinodal region
- Right: n_q = 0.4/fm^3, T = 20 Mev, inside spinodal region; large density fluctuations appear due to growth of unstable modes
- Colored regions correspond to N_q > 0.6/fm^3

Summary

- Coalescence model gives similar light nuclei yields in HIC as the thermal model if their binding energies are small compared to the temperature of the hadronic matter and their thermal wave lengths are much smaller than their sizes. Both results are similar to that from transport model studies in which deuterons are assumed to remain bounded and can be produced and dissociated.
- Coalescence model can naturally explain the suppressed production of light nuclei in collisions of small systems.
- Hypertriton is expected to be produced significantly later after nucleons and lambda have frozen out because of its large size and small binding.
- Nucleon density fluctuations enhance the production of light nuclei, providing a possible explanation for the experimental observations at SPS and RHIC.
- Understanding how quark density fluctuations due to the spinodal instability in baryon-rich quark matter can survive during hadronic evolution remains a challenge.